



MIIdAS—Multi-scale bias AdjuStment

Peter Berg^{1,*}, Thomas Bosshard^{1,*}, Wei Yang^{1,*}, and Klaus Zimmermann^{1,*}

¹Swedish Meteorological and Hydrological Institute, Folkborgsvägen 17, 601 76 Norrköping, Sweden

*These authors contributed equally to this work.

Correspondence: Peter Berg (peter.berg@smhi.se)

Abstract. Bias adjustment is the practice of statistically transforming climate model data in order to reduce systematic deviations from a reference data set, typically some sort of observations. There are numerous proposed methodologies to perform the adjustments – ranging from simple scaling approaches to advanced multi-variate distribution based mapping. In practice, the actual bias adjustment method is a small step in the application, and most of the processing handles reading, writing and linking different data sets. These practical processing steps become especially heavy with increasing model domain size and resolution in both time and space. Here, we present a new implementation platform for bias adjustment, which we call MIIdAS (Multi-scale bias AdjuStment). MIIdAS is a modern code implementation that supports features such as: modern Python libraries that allow efficient processing of large data sets at computing clusters, state-of-the-art bias adjustment methods based on quantile mapping, "day-of-year" based adjustments to avoid artificial discontinuities, and also introduces cascade adjustment in time and space. The MIIdAS platform has been set up such that it will continually support development of methods aimed towards higher resolution climate model data, explicitly targeting cases where there is a scale mismatch between data sets. The paper presents a comparison of different quantile mapping based bias adjustment methods and the subsequently chosen code implementation for MIIdAS. A current recommended setup of the MIIdAS bias adjustment is presented and evaluated in a pseudo-reference setup for regions around the world. Special focus is put on preservation of trends in future climate projections, and it is shown that the cascade adjustments perform better than the standard quantile mapping implementations, and often similar to more advanced trend preserving methods. The code is available from (Berg et al., 2021).

1 Introduction

Bias adjustment is commonly applied to adjust results from climate models to make them compatible with impact models and for calculations of climate indicators (e.g. Teutschbein and Seibert, 2012; Maraun et al., 2017). The issue with using climate model data directly arise from systematic deviations at regional and seasonal scales in climate models compared to observations. The core of a bias adjustment is therefore an algorithm that transforms the model values toward a reference. Because typical bias adjustment tools are pure statistical processors that can reshape almost any timeseries to look like the target reference (Maraun et al., 2017), it is important to be aware of side effects of the adjustment.

The mythological king Midas wished for his touch to become a powerful transfer function that converts any physical object to gold. Indeed, he was granted this wish, and his touch was the first great example of bias adjustment.



Gold! glorious gold! I am made up of gold!

I pluck a rose, a silly, fading rose,

Its soft, pink petals change to yellow gold;

Its stem, its leaves are gold—and what before

30 *Was fit for a poor peasant's festal dress*

May now adorn a Queen.

– Shelley (1922)

Of course, he soon realized his folly and narrow minded reference, which although useful for one purpose, was devastating for many other.

35 *...this meat*

which by its scent quickened my appetite

Has lost its scent, its taste,—'tis useless gold.

Alas! my fate! 'tis gold! this peach is gold

This bread, these grapes & all I touch! this meat

40 *Which by its scent quickened my appetite*

Has lost its scent, its taste,—'tis useless gold.

– Shelley (1922)

King Midas' pioneering career as a bias adjuster quickly fell apart after this initial failure. Thousands of years and another reality later, bias adjustment was picked up by the climate community. Several decades of step-wise improvements has significantly advanced the research field. From the first tools of mean bias adjustment through the delta change approach (e.g. Gleick, 1986), methods have evolved to more complex methods that account for complete distributions of a variable (e.g. Wood et al., 2002; Piani et al., 2010), multi-variate adjustments (Piani and Haerter, 2012; Vrac and Friederichs, 2014), temporal resolution (Haerter et al., 2010), spatial mismatch with observations (Haerter et al., 2015), to name some advancements. Adjustments are often applied to smaller regions, e.g. for a local impact model, where the range of values and climate regimes is constrained. However, employing bias adjustment across the globe has lead to a significant stress test of methods to, e.g., very dry climates, and regions of strong orography (Pechlivanidis et al., 2016; Photiadou et al., 2021). Further, a global reference data set can vary greatly in quality across the world, mainly as a consequence of available observational data (Berg et al., 2021; Hassler and Lauer, 2021).

The story of king Midas also teaches us to be aware of how the bias adjustment acts on scales beyond our main focus. Haerter et al. (2010) identified the potential interaction between statistics at different temporal time frames. They introduced the concept of "cascade bias adjustment" by separately applying bias adjustment to monthly mean data and daily anomalies, which are later merged to form the final adjusted timeseries. The motivation for the cascade method is to avoid introducing bias in one temporal resolution while adjusting another, which can occur in cases with bias in variance. The spatial character of the climate model and the observation was explored by Berg et al. (2015) for situations where the climate model has finer resolution



60 than the reference. They presented a method where a "pseudo-reference" was produced by merging model and observations, such that coarse scales agree with the reference and the finer spatial anomalies are added to this coarse background. The two approaches can be connected by applying a spatial cascade, where a coarse spatial resolution and finer scale anomalies are adjusted separately, or only one of the scales is adjusted. This can be useful in cases where the observational reference is of coarser resolution than the model; something which will likely become more common as model resolution increases.

65 Here we present a new take on king Midas attempts, by introducing MIdAS (Multi-scale bias AdjuStment). MIdAS is a bias adjustment software based on empirical quantile mapping, which for the first time introduces cascade adjustment in time and space, as an option to standard bias adjustment. Further, to avoid artificial discontinuities between calendar months, MIdAS makes use of day-of-year scaling steps. To balance the increased computational costs that comes with the day-of-year and multiple cascades, a significant effort has been put into multi-processing methods to allow scaling of the calculations on large
70 computational clusters. MIdAS is therefore coded in Python 3, using libraries well adapted to large computing clusters and automatic parallelization. The emphasis on large-scale application of the code separates MIdAS from most earlier published bias adjustment codes with focus mainly on presenting the method, and not on the practical usage.

In this paper, we present MIdAS with its main methods, assumptions and configurations, as well as a comprehensive evaluation and model intercomparison of MIdAS and other state-of-the-art methods, including several trend preserving methods.
75 Using a pseudo-reality setup with know modelled future pseudo-observations, the impact of the different bias adjustment methods are compared for various statistics. We especially address the cascade adjustments for time and space, and for different variables, and compare with published quantile mapping (QM) methods.

2 Bias adjustment methods

2.1 MIdAS method description

80 Although the core of the MIdAS method is the bias adjustment step, there are necessary preparations of data before and after that step, which demands careful and quality assured processing. Further, increasing domain and ensemble sizes put higher demand on the performance and scalability of the bias adjustment software. For these reasons, MIdAS is making use of the IRIS (Iris , 2021) library for reading CF-convention based Earth science data in the netcdf format, and Dask (Dask , 2016) for parallelized computations.

85 The core method of bias adjustment in MIdAS is an empirical quantile mapping (EQM). The basic requirements are a reference timeseries x , typically from observations, and a model timeseries y . A sub-period is defined for calibrating the bias adjustment, e.g. 1971–2000. Because bias often differs between seasons, the timeseries are split in smaller sections depending on the time of the year. Most methods do this by calendar month, but in MIdAS we opt for an approach where a window around each day of the year ($doy = [1, 365]$) is chosen. The standard setting is to use 15 d before and after, such that 31 d are used to
90 build the distribution of the reference and model data, specifically for each doy . Leap days are not explicitly handled, and the doy is defined from the first of January and counts the days until 365 is reached. Therefore, the 31st of December on leap years is not included, but will be bias adjusted with the same parameters as $doy = 365$.



In standard QM, the cumulative distribution functions (CDFs) of the reference dataset $F_{x,doy(i)}$ and of the model dataset $F_{y,doy(i)}$ are used to calculate the bias adjusted value z_i from the original value y_i according to Eq. 1.

$$\begin{aligned} z_i &= F_{x,doy(i)}^{-1}(F_{y,doy(i)}(y_i)) \\ 95 \quad &= (F_{x,doy(i)}^{-1} \cdot F_{y,doy(i)})(y_i) \end{aligned} \quad (1)$$

In practice, the CDFs are unknown and must be approximated. For EQM, this is done by the empirical cumulative distributions functions with linear interpolation between neighboring data points to avoid unphysical jumps. Since the number of data points defining the approximated CDFs is the same for reference and model due to our selection of points, we can pair them to form the points in the so-called Q-Q plot, which sorts the data in ascending order and plots them against each other, see Fig. 1. If we perform linear interpolation between these points and call the resulting function f , we see that this is identical to the EQM approach, i.e.

$$F_{x,doy(i)}^{-1} \cdot F_{y,doy(i)} = f_{doy(i)}. \quad (2)$$

The main downside of the EQM approach is its use of resources. Due to the relatively large number of points, a commensurate amount of storage is needed because all points of the calibration dataset must be stored as parameters for the bias adjustment. Furthermore, the evaluation of the adjustment function becomes more costly as more points (longer reference period, longer time window) are considered since the relevant pair of data points must be located first. This is done to diminishing returns because generally speaking, the vast majority of points falls into the same central interval, doing little to improve the quality of the adjustment.

Our goal with MIDAS is to find a good approximation for f that does not suffer from these problems and offers better resource efficiency and scalability. We achieve this by fitting a linear smoothing spline function to the Q-Q plot, using the routine `splrep` from Virtanen et al. (2020), which in turn is based on the FITPACK routines by Paul Dierckx (Dierckx, 1975, 1981, 1982, 1995). This approach allows a good approximation of f with far fewer knots in the spline, while still guaranteeing a good representation of all data points. It is tempting to go to higher order, e.g. cubic, splines to achieve an even better and smoother representation, possibly with even fewer knots. However, experience shows that this can introduce overshooting behavior, particularly at the ends of the interval, whereas linear splines give a faithful reflection of the calibration data.

The spline fitting function also provides us with the possibility of using weights for individual data points. We use this to mitigate the following problem.

Earlier studies have shown the sensitivity of such EQM approaches regarding the tail behaviour (Switanek et al., 2017). To avoid excessive impact from outliers in the tails, a linear function is fitted to the 90% most central data points of the Q-Q plot. The weights to the spline function are then defined according to the standard deviation of the data points from the linear fit. To avoid excessive weights for individual points, a minimal standard deviation of 1% of the midpoint of all reference values with a minimum of a 1% weight per point so that no single points will receive a too large weight. When the splines have been fitted for each doy , each data point of the model timeseries will be adjusted according to its value and doy according to:

$$z_i = f_{doy(i)}(y_i), \quad (3)$$



125 where z_i is the bias adjusted data for time step i . The scaling is as also outlined in red in Fig. 2.

In the case of a time cascade adjustment, we follow the method as outlined in Haerter et al. (2010) and extend it to include also a multiplicative case. Each timeseries is first split up in two separate timeseries:

$$x_i = x'_i + \overline{x_i}, \quad (4)$$

130 where i is the timestep in days, and the two cascades are indicated by an overbar for the coarser temporal aggregation, e.g. $\overline{x_i} = \sum_{k=i}^{i+30} x_k$, and a prime for anomalies thereof. The model timeseries, y is split up in the same way. Equation 4 is applied to non-bounded variables such as temperature that can handle such additive splitting. For bounded variables, such as precipitation, the separation is instead multiplicative:

$$x_i = x'_i \cdot \overline{x_i}. \quad (5)$$

135 One can now chose to separately adjust each of the cascades, and then return the final bias adjusted timeseries by substituting for z in Eq 4.

Albeit not implemented in MIdAS itself, experiments using a spatial cascade has been performed in research projects using pre- and postprocessing. The spatial cascade follows similar form as the temporal, but is based on a coarse and a finer scale spatial resolution. with an additive of multiplicative connection as for the temporal cascades.

140 We are here addressing bias adjustment of daily mean temperature and precipitation. Whereas temperature follows the steps outlined above, an additional step is introduced for precipitation to adjust the number of wet days. MIdAS employs the SSR (Singularity Stochastic Removal) method for wet day adjustments (Vrac et al., 2016). SSR works in four steps:

1. Find the threshold lowest precipitation value, P_{th} , greater than zero across both timeseries.
2. Set all zero values to a random number in the range $(0, P_{th})$.
3. Let the bias adjustment step assign new values to the timeseries, including the values promoted from zero in step 2.
- 145 4. Finally, all values below P_{th} are set to zero.

Together with the quantile mapping, SSR will ensure that the number of wet days are close to the reference data both when the bias is wet and dry. However, any removed excessive, or promoted dry, time step will hold ny physical meaning in themselves. This is still a reasonable methodology since these values are normally only affecting the lower end of the precipitation distribution.

150 2.2 Additional methods for bias adjustment

To put MIdAS' performance in context, other often cited and used methods from different flavours of QM are included in the evaluation (see also Fig. 2). The included methods are of an empirical nature, and we have on purpose left out parametric methods such as ISIMIP3 (Lange, 2019) and DBS (Yang et al., 2010) due to difficulties in identifying the appropriate distribution functions for different cascades.



155 **qmapQ** Empirical quantile mapping (EQM) considers each single data point in F , which works well in the thicker centre of
the distributions. However, the methods becomes more sensitive at the tails. Switanek et al. (2017) showed that if the
sensitivity to outliers in the tails is not addressed, it can have severe impacts when applied in another climate period. This
issue has been dealt with in different ways, and here we used the method we call "qmapQ" from (Gudmundsson et al.,
2012), which divides the data range in one hundred quantile steps, which ensures equal number of data points in each
160 sample. Both temperature and precipitation are treated equally. The correction found for the highest quantile is used to
estimate those larger than the training values. We use the qmap library in R (Gudmundsson, 2016).

DQM by Cannon et al. (2015), performs a first step of detrending the timeseries for the mean value. An EQM is then applied,
after which the trends are added to the bias adjusted data. The trends are calculated as discrete differences between
30-year time slices of the models for a future and a historical reference period, see Section 2.3.

165 **QDM** by Cannon et al. (2015) follows the same basic principles as EQM, but instead of initiating the transformation by the
value, it originates from the quantile value of F . This gives the same result as EQM for the reference period, but may
differ for other periods. Here, we calculate the future distribution for set time-slices of the investigated periods. QDM
further removes a linear trend before the bias adjustment step, and adds it back afterwards, in order to retain the original
climate signal.

170 **CDF-t** by Michelangeli et al. (2009) is a more intricate method which uses an estimated future reference distribution for the
adjustment. In a first step, and adjustment is made at the quantile level, as in QDM, and a pseudo-future observation is
constructed. The implementation in the R-package "CDFt" is used (Vrac and Michelangeli, 2009).

2.3 Evaluation scheme

We make use of the so-called pseudo-reality approach of evaluating the bias adjustment methods (Maraun, 2012). In pseudo-
175 reality, a model ensemble with a historical and future projection is employed. Each model will in turn be given the role of the
pseudo-observations, i.e. to act as the reference for the bias adjustment of the other models. Calibration of the bias adjustment
methods is performed for the period 1971-2000, and then applied to the periods 1971-2000, 2011-2040, 2041-2070, and 2071-
2100.

2.4 Evaluation parameters and ranking

180 All statistics are calculated for each calendar month, and across 30-year time-slices. The statistic operators, O , include: the
mean, the 0, 1, 99 and 100th percentiles, the number of wet days (for precipitation), and the PDF (probability density function)
skill score (pdfSS). pdfSS is defined as the overlapping area of two PDFs, which leads to a value 0 for no overlap to 1 for a
perfect overlap. The bias, β is calculated for all but pdfSS, for each month m , climate model i and grid point g in a domain:

$$\beta_g(m, i) = O_{mod, g}(m, i) - O_{ref, g}(m). \quad (6)$$



Table 1. Description of the ranking methods.

Method	Description
1	Ranking across all ensemble members, regions, periods and months.
2	Ranking for ensemble mean of all ensemble members, averaged over all periods and months. Then the ranks are averaged across all domains.
3	Ranking for ensemble median, averaged over all periods and months. Then the ranks are averaged across all domains.

185 The bias is summarized per domain (averaging operator " $\langle \rangle_z$ ") as an absolute bias:

$$\beta = \langle |\beta_g(m, i)| \rangle_g \quad (7)$$

One can expect β to be close to zero in the calibration period, but is likely non-zero for other periods. A basic assumption of the bias adjustment methods is that of time-stationarity in model bias, which means that the remaining bias outside the calibration period should preferably be low and near constant. The impact of the bias adjustment on the climate change signals,

190 Δ is investigated similarly as the bias:

$$\Delta_g = O_{mod,g}(m, i) - O_{ref,g}(m, i) \quad (8)$$

and

$$\Delta = \langle \Delta_g(m, i) \rangle_g . \quad (9)$$

195 Three different ranking methods are then calculated, see Tab. 1. The statistics entering the ranking can be β for the different statistics (low values for good performance, except pdfSS for which high values marks good performance), or the modification of the climate change signal Δ . For the latter, one often strives to reduce impacts of the bias adjustment on the climate change signal. However, detailed studies of how models through poorly simulated physical processes lead to bias can justify the bias adjustment method to affect the change signal. We do not go into such depth in the current evaluation.

3 Data

200 Five global climate models (GCMs) are included in the study, see Tab. 2. The models were chosen based on an ensemble of opportunity of 18 GCMs from which 4 models were chosen such that they were as far apart as possible according to the model genealogy by (Knutti et al., 2013) based on the projection changes under RCP8.5. It was assumed that the further



Table 2. List of the CMIP-5 GCMs included in the evaluation along with their RIP (realisation-initialization-physics) code. All GCMs were first remapped to a common 2 degree grid regular longitude-latitude grid.

GCM	RIP
NorESM1-M	r1i1p1
IPSL-IPSL-CM5A-MR	r1i1p1
Inmcm4	r1i1p1
MPI-M-MPI-ESM-MR	r1i1p1

away the models are according to the genealogy, the more independent they are. Model independence is a desired feature in a pseudo-reality experiment.

205 The evaluation is for computational reasons limited to a selection of ten regions around the world, see Fig. 3. The regions were chosen based on personal experience with previous applications of bias adjustment with issues such as inflation of variance (NAM_1), dry regions (AFR_1), heavy precipitation (AFR_2, SAM_2), monsoon (WAS_1), strong land-sea contrasts (EAS_1, SAM_1) different challenging climates for the models (AUS_1, ARC_1), or simply locations of particular interest (EUR_1).

4 Results

210 4.1 Temporal cascade adjustments

In a first study, the temporal cascade is investigated for three different methods: QDM, DQM, and qmapQ. The SSR method was employed to adjust wet days for all methods, and in the cascade case it is applied before the timeseries is split into the cascades. Each model performs two experiments: a baseline without cascade adjustment, and an experiment including two cascades at 31-day coarse temporal resolution and its daily anomalies. Figures 4 and 5 show the resulting median bias across
215 all ensemble members in the pseudo-reality setup, with the different geographical regions on the vertical axis, and separately for each month of the year on the horizontal axis. Bias is normalised per regions because the bias can differ substantially for precipitation. Figure 4 shows that all methods succeed in substantially reducing the bias for mean temperature. QDM leads in all three ranking methods, and performs slightly worse in the cascade mode. qmapQ and DQM follows closely, with qmapQ_casc consistently outperforming the baseline qmapQ. However, DQM and QDM perform worse with the cascade option.

220 For precipitation (Fig. 5), qmapQ and qmapQ_casc consistently outperform the other methods for all regions and all rankings. DQM performs generally well, but suffer from some outlier bias for certain regions and months. We did not go into closer evaluation of the reasons, other than verifying that the method is correctly implemented and that the issues lie with the methods themselves. Although not seen in the presented statistics, qmapQ_casc can for some regions and seasons lead to strong remaining bias compared to the other methods. This is likely a consequence of the multiplicative cascade used for precipitation, e.g.



225 by multiplying two small values. Because bias adjustment is often part of a process chain to achieve an assessment of impact of climate change, such uncertainty in the results is problematic.

In conclusion, the evaluation of the cascades have shown promise for both variables with the qmapQ method, but less so for the other bias adjustment methods. Further work on constraining the cascades for precipitation is needed, and we therefore decided to proceed with using a temporal cascade only for temperature, whereas precipitation adjustments are based on the original daily data. Temperature is also the variable with the strongest increase as a result of climate change, and therefore with
230 the most likely potential of destructive interference between the temporal scales (Haerter et al., 2010).

4.2 Method inter-comparison

Based on the initial results on the cascade method presented in Section 4.1, the MIdAS bias adjustment method was implemented using a cascade of 31-day means and daily anomalies for temperature, and a single absolute daily data adjustment
235 for precipitation. Here, MIdAS is compared with the methods listed in Section 2.2, with each method in its standard settings, except for qmapQ which is accompanied by the cascade version qmapQ_casc used in Section 4.1. It should be noted upfront that MIdAS differs from the other methods by the running window approach, compared to other methods' discrete steps on calendar months when calculating the transfer functions. The implication is that MIdAS will suffer in the calendar month-based statistical analysis, which should be kept in mind when evaluating its performance.

240 All methods are implemented using the SSR method for wet day adjustments, with exception of the CDF-t method, which has its own built-in adjustment.

The pseudo-reality evaluation is performed through analysis of summary statistics as presented in Fig. 6–9. Each figure presents an overview of the different analysed regions, for all time periods, and all calendar months of the year, and for each bias adjustment method. Further, each plot is accompanied by the ranking scores, where the summary ranking 1 (see
245 Section 2.4) is presented for all statistics in Tab. 3 and Tab. 4. The data are normalised per region for presentation clarity, and presented separately for bias, β , and impact on the climate change signal, Δ .

4.2.1 Precipitation

Fig. 6 shows the results on bias for mean precipitation. The most striking feature of this figure is that all methods generally succeed in reducing the original bias of the models (leftmost column). However, there are some exceptions where different
250 methods fail, and even increase the bias, e.g. CDF-t in AFR_1 and SAM_1, and DQM in AFR_1. The rankings indicate qmapQ, qmapQ_casc and MIdAS as top three performers, with QDM advancing before MIdAS for ranking 3. These four methods perform rather similarly to each other.

Table 3 presents a summary of ranking 1 for all statistics. MIdAS is always in top three of the methods, with scores close to the better ranking methods. Considering that MIdAS suffers from its running mean temporal window in this comparison, its
255 performance can be considered to be at least on par with qmapQ, qmapQ_casc and QDM. Notably, MIdAS's performance for maximum precipitation is high, whereas the otherwise top scoring methods qmapQ_casc and QDM perform worse.



Table 3. Bias as calculated in ranking 1, across all regions, time periods and months. Occasions where the statistic was strongly affected by outliers is marked "inf", for infinity.

Variabel(statistic)	uncorr	MIIdAS	qmapQ_casc	qmapQ	QDM	CDF-t	DQM
P(min)	0.08	0.04	0.04	0.04	0.04	0.04	inf
P(mean)	1.39	0.47	0.43	0.43	0.53	0.56	inf
P(99p)	7.99	3.10	4.14	3.08	3.27	3.66	inf
P(max)	17.69	10.20	14.31	9.41	11.12	10.43	inf
P(pdfSS)	0.75	0.89	0.89	0.89	0.88	0.81	0.87
T(min)	3.83	1.89	1.51	1.4	1.55	1.77	1.47
T(1p)	3.44	1.23	1.09	1.11	1.01	1.1	1.06
T(mean)	2.88	0.82	0.83	0.93	0.8	0.82	0.82
T(99p)	2.86	1.35	1.29	1.16	1.04	1.12	1.06
T(max)	2.96	1.76	1.6	1.26	1.23	2.69	1.15
T(pdfSS)	0.5	0.78	0.78	0.76	0.78	0.78	0.78

Table 4. Modulation of the climate change signal as calculated in ranking 1, across all regions, time periods and months. The method with the overall lowest impact on the signal for each statistics is emphasised with a bold font. Occasions where the statistic was strongly affected by outliers is marked "inf", for infinity.

Variabel(statistic)	MIIdAS	qmapQ_casc	qmapQ	QDM	CDF-t	DQM
P(min)	0.07	0.04	0.04	0.03	0.46	inf
P(mean)	0.17	0.14	0.17	0.22	0.15	inf
P(99p)	1.49	1.32	1.6	1.17	1.16	inf
P(max)	2.60	3.31	1.41	5.22	2.32	inf
T(min)	0.67	0.7	0.99	0.07	0.83	0.53
T(1p)	0.54	0.57	0.79	0.03	0.35	0.25
T(mean)	0.42	0.43	0.58	0	0.1	0
T(99p)	0.41	0.33	0.42	0.02	0.26	0.21
T(max)	0.51	0.33	0.02	0.17	2.24	0.66

The impact of the different methods on the climate change signal is presented for mean precipitation in Fig. 7. By visual inspection, MIIdAS performs similarly to qmapQ and qmapQ_casc. Some more prominent differences are visible for AFR_2 in the beginning of the year. Whereas most methods have a generally amplifying impact on the climate change signal, the CDF-t



260 method is reducing the magnitude of the changes. DQM has generally lower impacts, but also suffers from producing outliers
in some cases, which impact strongly on the ranking statistics. The top three ranking methods, i.e. those with the smallest
impact on the change signals, are qmapQ_casc, CDF-t and qmapQ. In fourth place is MIDAS, followed by the QDM and DQM
methods. It is interesting that the trend preserving methods QDM and DQM perform worse in this comparison.

The results are fairly consistent with the above conclusions across the other statistics, as shown for ranking 1 in Tab. 4. The
265 main differences is the better performance of QDM for minimum and 99p precipitation, and the better performance of MIDAS
for 99p and maximum precipitation.

4.2.2 Temperature

Figure 8 shows that the mean temperature is, like mean precipitation, well adjusted by all methods. The only strong outstanding
features are from qmapQ in ARF_1, and qmapQ_casc at the end of the year in ARC_1. QDM is clearly outperforming all other
270 methods, with top scores in each ranking. However, the differences are very small between QDM, CDF-t and MIDAS, whereas
DQM and the qmapQ methods perform only slightly worse.

Ranking 1 in Tab. 3 shows that QDM is also the overall best method for the different statistics. The differences are, however,
very small across the different methods - often between 0.1 – 0.5 °C. This can be considered small compared to the original
bias of 2.9 to 3.8 °C.

275 Regarding the impact on the climate change signal, the initial detrending performed in QDM results in non-existing or very
small impacts on the mean, see Fig. 9. Also DQM and CDF-t explicitly account for the climate change signal, and have low
impacts on the signal for mean temperature. However, Tab. 4 reveals that the impact is stronger on other statistics that are
not explicitly accounted for - most notably minimum and maximum temperature. Again, QDM is keeping the impact on the
climate change signal low and gets the overall best ranking, followed by DQM. CDF-t suffers from some larger outliers for
280 minimum, and especially maximum temperature of several degrees Celsius. qmapQ, qmapQ_casc and MIDAS are free to affect
the change signal, but still remain at less than one degree Celsius, and often below 0.5 °C. qmapQ_casc has consistently lower
impacts on the signal than qmapQ, which is expected (Haerter et al., 2010), and MIDAS is overall on par with qmapQ_casc.

4.3 Discussion

The idea behind the development of MIDAS was to primarily have a good platform to build bias adjustments methods on.
285 The envisioned future applications of bias adjustment is on scales that reach beyond the resolution in both time and space of
today's gridded observations. Therefore, it is necessary to be able to perform adjustments on resolutions where one have trust
in the observations. As previously argued for by Berg et al. (2015), bias adjustment should avoid tampering with scales better
simulated by the dynamic models. Many gridded data sets have different "models" for mapping, e.g., orographic and other
effects on precipitation. Such models are not necessarily better than the dynamical model's representation, and should therefore
290 not obviously be imposed in a bias adjustment process. Spatial cascades can circumvent this issue, by e.g. only performing
adjustment on a coarser scale. One example where MIDAS was applied in such a context was for a recent bias adjustment
of downscaled CMIP6 data for the Mashreq domain. The reference observations used were at 25 km resolution, whereas the



295 downscaled models were at 12.5 km resolution. A spatial cascade was then used to only adjust temperature at a coarsened spatial resolution, by employing a 3x3 grid point filter on the data, and then adding the original fine scale anomalies to the bias adjusted cascade. For precipitation, there are still some caveats to work out for the cascades. Because of the multiplicative "nature" of this zero-bounded variable, the cascade can lead to exaggerated response when multiplying small numbers. It is therefore necessary to add constraints on the data.

300 Most bias adjustment approaches are implemented to be applied by calendar month. This can introduce significant unphysical steps in the timeseries between different months. The day-of-year 31-day window used in MIdAS avoids this issue, but at a computational cost with more than 30 times the number of calculations for the calibration. The higher detail in this approach improves the bias adjustment. However, using standard evaluation on calendar months, the method will appear to perform worse as the results within a month is based on statistics overlapping parts of multiple calendar months. This must be kept in mind when performing inter-comparison evaluations of bias adjustment methods.

5 Conclusions

305 The MIdAS model for bias adjustment was presented. Currently, the core functions of bias adjustment is similar to other released EQM methods, and the implementation of MIdAS performs on par with or better than the selection of state-of-the-art methods included in the evaluation.

Further, MIdAS features some additions that are new to released bias adjustment software:

- 310 – cascade adjustments to separately bias adjust a coarse scale, and smaller scale anomalies. This is implemented for temporal cascades in the code, and can be performed by pre- and post-processing for spatial cascades as well.
- day-of-year running window to build the transfer function, rather than the standard calendar month discrete steps. This removes potential nonphysical steps between adjacent days in different months.

The processing platform of MIdAS has been constructed for adding features such as multi-cascade (time and space "scale") and multi-variate bias adjustment methods. This makes MIdAS a good base to build future development of bias adjustment on.

315 *Code and data availability.* The code for the presented version of MIdAS is available at <https://doi.org/10.5281/zenodo.5989710> under the GNU LESSER GENERAL PUBLIC LICENSE v3. The repository includes documentation of the method, automatic set up scripts for a conda environment to run the model, and information on how to apply it. All climate model data used in the pseudo-reality experiments were downloaded from the ESGF (Earth System Grid Federation) nodes. The scripts for producing the inter-comparison of bias adjustment methods and the analysis are available from <https://doi.org/10.5281/zenodo.6043222> (Berg et al., 2022). The repository also contains the
320 remapped excerpts of the global climate models and the resulting files from the bias adjustments that are presented in the paper.



Author contributions. PB was leading the method development, and contributed to the experiments. TB set up the experiment design and carried out the evaluation. WY implemented the method-intercomparison and carried out the experiments. KZ performed the MIdAS technical implementation and code design. PB prepared the manuscript, with contributions from all co-authors.

Competing interests. The authors declare that they have no conflicts of interest.

325 *Acknowledgements.* The development of MIdAS was supported by SMHI and the project DIRT-X. DIRT-X is part of AXIS, an ERA-NET initiated by JPI Climate, and funded by FFG Austria, BMBF Germany, FORMAS Sweden, NWO NL, RCN Norway with co-funding by the European Union (Grant No. 776608). We would especially like to thank our SMHI colleagues Lars Barring, Yeshewatesfa Hundecha, Magnus Hieronymus, Marco Kupiainen, Grigory Nikulin, Elin Sjökvist and Renate Wilcke for useful discussions and inputs on the development of MIdAS.



330 References

- Berg, P., Bosshard, T., and Yang, W.: Model Consistent Pseudo-Observations of Precipitation and Their Use for Bias Correcting Regional Climate Models, *Climate*, 3, 118–132, <https://doi.org/10.3390/cli3010118>, 2015.
- Berg, P., Almén, F., and Bozhinova, D.: HydroGFD3.0 (Hydrological Global Forcing Data): a 25 km global precipitation and temperature data set updated in near-real time, *Earth System Science Data*, 13, 1531–1545, <https://doi.org/10.5194/essd-13-1531-2021>, 2021.
- 335 Berg, P., Bosshard, T., Yang, W., and Zimmermann, K.: MIDAS (Multi-scale bias AdjuStment), Zenodo, <https://doi.org/10.5281/zenodo.5989710>.
- Berg, P., Bosshard, T., and Yang, W.: MIDAS: Bias adjustment inter-comparison and evaluation scripts, Zenodo, <https://doi.org/10.5281/zenodo.6043222>.
- Cannon, A. J., Sobie, S. R., and Murdock, T. Q.: Bias Correction of GCM Precipitation by Quantile Mapping: How Well Do Methods
340 Preserve Changes in Quantiles and Extremes?, *Journal of Climate*, 28, 6938–6959, <https://doi.org/10.1175/jcli-d-14-00754.1>, 2015.
- Dask Development Team. Dask: Library for dynamic task scheduling URL <https://dask.org>, 2016
- Dierckx, P.: An algorithm for smoothing, differentiation and integration of experimental data using spline functions, *Journal of Computational and Applied Mathematics*, 1, 165–184, [https://doi.org/10.1016/0771-050x\(75\)90034-0](https://doi.org/10.1016/0771-050x(75)90034-0), 1975.
- Dierckx, P.: An improved algorithm for curve fitting with spline functions, TW Reports, Department of Computer Science, K.U. Leuven,
345 Belgium, 1981.
- Dierckx, P.: A Fast Algorithm for Smoothing Data on a Rectangular Grid while Using Spline Functions, *SIAM Journal on Numerical Analysis*, 19, 1286–1304, <https://doi.org/10.1137/0719093>, 1982.
- Dierckx, P.: Curve and surface fitting with splines, Oxford University Press, 1995.
- Gleick, P. H.: Methods for evaluating the regional hydrologic impacts of global climatic changes, *Journal of Hydrology*, 88, 97–116,
350 [https://doi.org/10.1016/0022-1694\(86\)90199-x](https://doi.org/10.1016/0022-1694(86)90199-x), 1986.
- Gudmundsson, L.: qmap: Statistical transformations for post-processing climate model output, r package version 1.0-4, 2016.
- Gudmundsson, L., Bremnes, J. B., Haugen, J. E., and Engen-Skaugen, T.: Technical Note: Downscaling RCM precipitation to the station scale using statistical transformations – a comparison of methods, *Hydrology and Earth System Sciences*, 16, 3383–3390, <https://doi.org/10.5194/hess-16-3383-2012>, 2012.
- 355 Haerter, J. O., Berg, P., and Hagemann, S.: Heavy rain intensity distributions on varying time scales and at different temperatures, *Journal of Geophysical Research*, 115, 7 pp., <https://doi.org/doi:10.1029/2009JD013384>, 2010.
- Haerter, J. O., Eggert, B., Moseley, C., Piani, C., and Berg, P.: Statistical precipitation bias correction of gridded model data using point measurements, *Geophys. Res. Lett.*, 42, 1919–1929, <https://doi.org/10.1002/2015GL063188>, 2015.
- Hassler, B. and Lauer, A.: Comparison of Reanalysis and Observational Precipitation Datasets Including ERA5 and WFDE5, *Atmosphere*,
360 12, 1462, <https://doi.org/10.3390/atmos12111462>, 2021.
- Iris: A Python package for analysing and visualising meteorological and oceanographic data sets, v1.2, 2010 - 2013, Exeter, Devon, <http://scitools.org.uk/>
- Knutti, R., Masson, D., and Gettelman, A.: Climate model genealogy: Generation CMIP5 and how we got there, *Geophysical Research Letters*, 40, 1194–1199, <https://doi.org/10.1002/grl.50256>, 2013.
- 365 Lange, S.: Trend-preserving bias adjustment and statistical downscaling with ISIMIP3BASD (v1.0), *Geoscientific Model Development*, 12, 3055–3070, <https://doi.org/10.5194/gmd-12-3055-2019>, 2019.



- Maraun, D.: Nonstationarities of regional climate model biases in European seasonal mean temperature and precipitation sums, *Geophysical Research Letters*, 39, 1–5, <https://doi.org/10.1029/2012gl051210>, 2012.
- Maraun, D., Shepherd, T. G., Widmann, M., Zappa, G., Walton, D., Gutiérrez, J. M., Hagemann, S., Richter, I., Soares, P. M. M., Hall, A., and Mearns, L. O.: Towards process-informed bias correction of climate change simulations, *Nature Climate Change*, 7, 764–773, <https://doi.org/10.1038/nclimate3418>, 2017.
- Michelangeli, P.-A., Vrac, M., and Loukos, H.: Probabilistic downscaling approaches: Application to wind cumulative distribution functions, *Geophysical Research Letters*, 36, <https://doi.org/10.1029/2009gl038401>, 2009.
- Pechlivanidis, I., Olsson, J., Bosshard, T., Sharma, D., and Sharma, K.: Multi-Basin Modelling of Future Hydrological Fluxes in the Indian Subcontinent, *Water*, 8, 177, <https://doi.org/10.3390/w8050177>, 2016.
- Photiadou, C., Arheimer, B., Bosshard, T., Capell, R., Elenius, M., Gallo, I., Gyllensvärd, F., Klehmet, K., Little, L., Ribeiro, I., Santos, L., and Sjökvist, E.: Designing a Climate Service for Planning Climate Actions in Vulnerable Countries, *Atmosphere*, 12, 121, <https://doi.org/10.3390/atmos12010121>, 2021.
- Piani, C. and Haerter, J. O.: Two dimensional bias correction of temperature and precipitation copulas in climate models, *Geophysical Research Letters*, 39, <https://doi.org/10.1029/2012gl053839>, 2012.
- Piani, C., Weedon, G., Best, M., Gomes, S., Viterbo, P., Hagemann, S., and Haerter, J.: Statistical bias correction of global simulated daily precipitation and temperature for the application of hydrological models, *Journal of Hydrology*, 395, 199 – 215, <https://doi.org/DOI:10.1016/j.jhydrol.2010.10.024>, 2010.
- Räisänen, J. and Räty, O.: Projections of daily mean temperature variability in the future: cross-validation tests with ENSEMBLES regional climate simulations, *Climate Dynamics*, 41, 1553–1568, <https://doi.org/10.1007/s00382-012-1515-9>, 2012.
- Räty, O., Räisänen, J., and Ylhäisi, J. S.: Evaluation of delta change and bias correction methods for future daily precipitation: intermodel cross-validation using ENSEMBLES simulations, *Climate Dynamics*, 42, 2287–2303, <https://doi.org/10.1007/s00382-014-2130-8>, 2014.
- Shelley, M. W.: *Proserpine & Midas : two unpublished mythological dramas*, Humphrey Milford, 1922.
- Switanek, M. B., Troch, P. A., Castro, C. L., Leuprecht, A., Chang, H.-I., Mukherjee, R., and Demaria, E. M. C.: Scaled distribution mapping: a bias correction method that preserves raw climate model projected changes, *Hydrology and Earth System Sciences*, 21, 2649–2666, <https://doi.org/10.5194/hess-21-2649-2017>, 2017.
- Teutschbein, C. and Seibert, J.: Bias correction of regional climate model simulations for hydrological climate-change impact studies: Review and evaluation of different methods, *Journal of Hydrology*, 456–457, 12–29, <https://doi.org/10.1016/j.jhydrol.2012.05.052>, 2012.
- Virtanen, P., Gommers, R., Oliphant, T. E., Haberland, M., Reddy, T., Cournapeau, D., Burovski, E., Peterson, P., Weckesser, W., Bright, J., van der Walt, S. J., Brett, M., Wilson, J., Millman, K. J., Mayorov, N., Nelson, A. R. J., Jones, E., Kern, R., Larson, E., Carey, C. J., Polat, İ., Feng, Y., Moore, E. W., VanderPlas, J., Laxalde, D., Perktold, J., Cimrman, R., Henriksen, I., Quintero, E. A., Harris, C. R., Archibald, A. M., Ribeiro, A. H., Pedregosa, F., van Mulbregt, P., Vijaykumar, A., Bardelli, A. P., Rothberg, A., Hilboll, A., Kloeckner, A., Scopatz, A., Lee, A., Rokem, A., Woods, C. N., Fulton, C., Masson, C., Häggström, C., Fitzgerald, C., Nicholson, D. A., Hagen, D. R., Pasechnik, D. V., Olivetti, E., Martin, E., Wieser, E., Silva, F., Lenders, F., Wilhelm, F., Young, G., Price, G. A., Ingold, G.-L., Allen, G. E., Lee, G. R., Audren, H., Probst, I., Dietrich, J. P., Silterra, J., Webber, J. T., Slavič, J., Nothman, J., Buchner, J., Kulick, J., Schönberger, J. L., de Miranda Cardoso, J. V., Reimer, J., Harrington, J., Rodríguez, J. L. C., Nunez-Iglesias, J., Kuczynski, J., Tritz, K., Thoma, M., Newville, M., Kümmerer, M., Bolingbroke, M., Tartre, M., Pak, M., Smith, N. J., Nowaczyk, N., Shebanov, N., Pavlyk, O., Brodtkorb, P. A., Lee, P., McGibbon, R. T., Feldbauer, R., Lewis, S., Tygier, S., Sievert, S., Vigna, S., Peterson, S., More, S., Pudlik, T., Oshima, T., Pingel, T. J., Robitaille, T. P., Spura, T., Jones, T. R., Cera, T., Leslie, T., Zito, T., Krauss, T., Upadhyay, U., Halchenko,



- 405 Y. O., and Vázquez-Baeza, Y.: SciPy 1.0: fundamental algorithms for scientific computing in Python, *Nature Methods*, 17, 261–272,
<https://doi.org/10.1038/s41592-019-0686-2>, 2020.
- Vrac, M. and Friederichs, P.: Multivariate—Intervariable, Spatial, and Temporal—Bias Correction, *Journal of Climate*, 28, 218–237,
<https://doi.org/10.1175/jcli-d-14-00059.1>, 2014.
- Vrac, M. and Michelangeli, P.-A.: CDFt: Downscaling and Bias Correction via Non-Parametric CDF-Transform, *r* package version 1.0.1,
410 2009.
- Vrac, M., Noël, T., and Vautard, R.: Bias correction of precipitation through Singularity Stochastic Removal: Because occurrences matter,
Journal of Geophysical Research: Atmospheres, 121, 5237–5258, <https://doi.org/10.1002/2015jd024511>, 2016.
- Wood, A. W., Maurer, E., Kumar, A., and Lettenmaier, D.: Long-range experimental hydrological forecasting for the eastern United States,
Journal of Geophysical Research, 107, 15pp., <https://doi.org/10.1029/2001JD000659>, 2002.
- 415 Yang, W., Andréasson, J., Graham, L. P., Olsson, J., Rosberg, J., and Wetterhall, F.: Distribution based scaling to improve us-
ability of regional climate model projections for hydrological climate change impacts studies, *Hydrol. Res.*, 41.3-4, 211–229,
<https://doi.org/10.2166/nh.2010.004>, 2010.

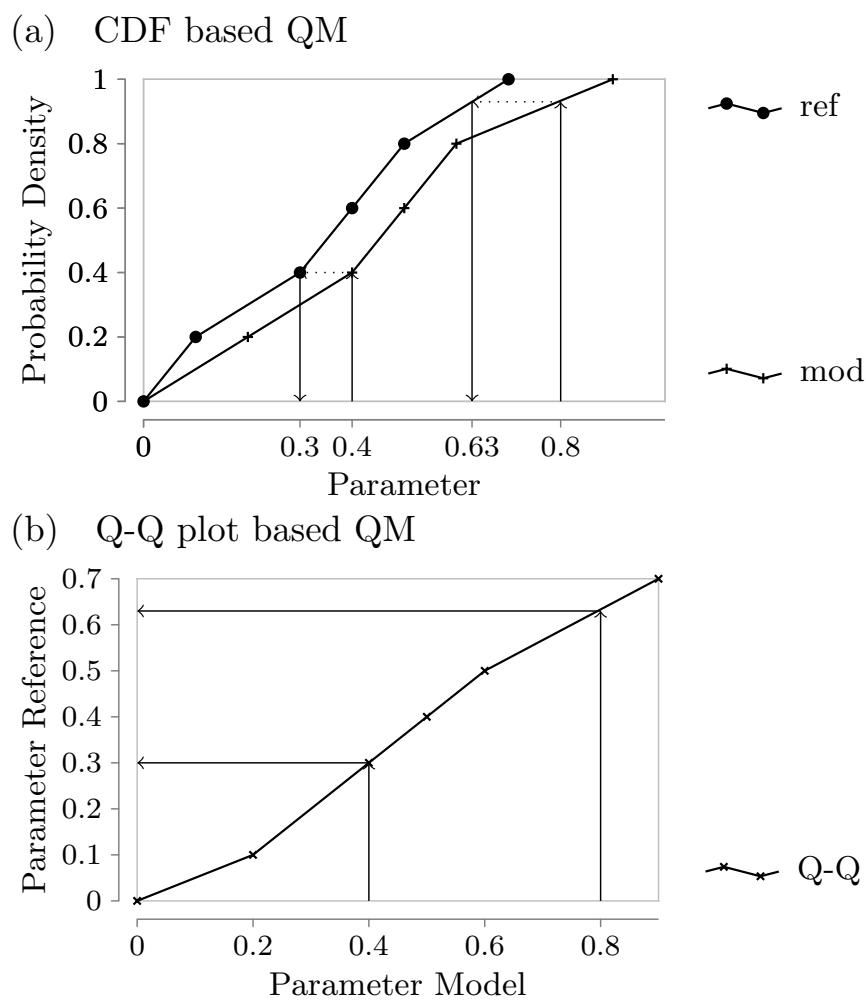


Figure 1. Illustration of the equivalence of CDF based EQM and Q-Q plot based EQM. In (a) we plot the linear interpolation version of the empirical CDFs for two example datasets, while (b) shows the Q-Q plot that results from the same data.

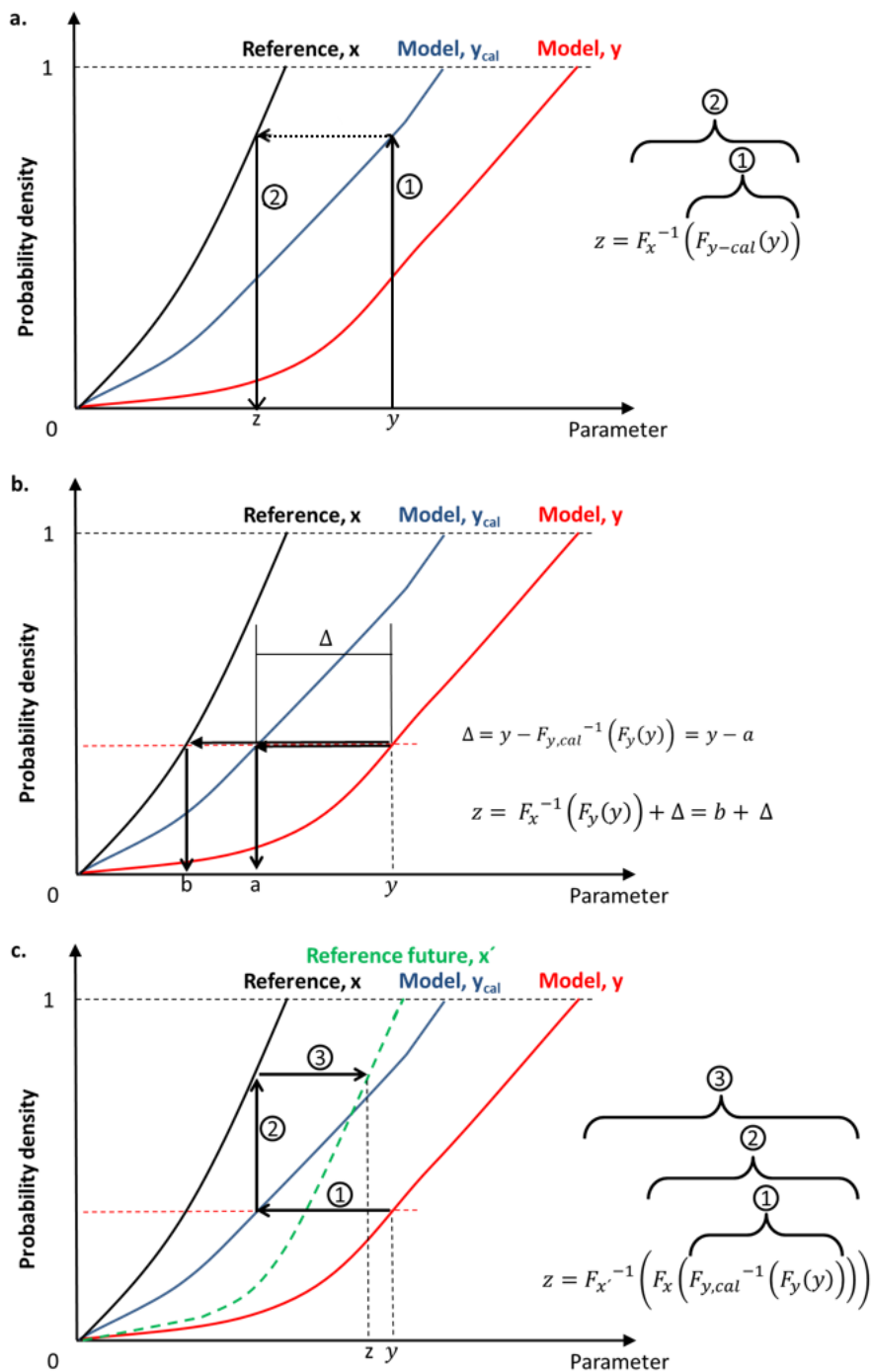


Figure 2. Descriptive visualisation of the quantile mapping for (a) MIDAS, EQM, and DQM, (b) QDM, and (c) CDF-t.

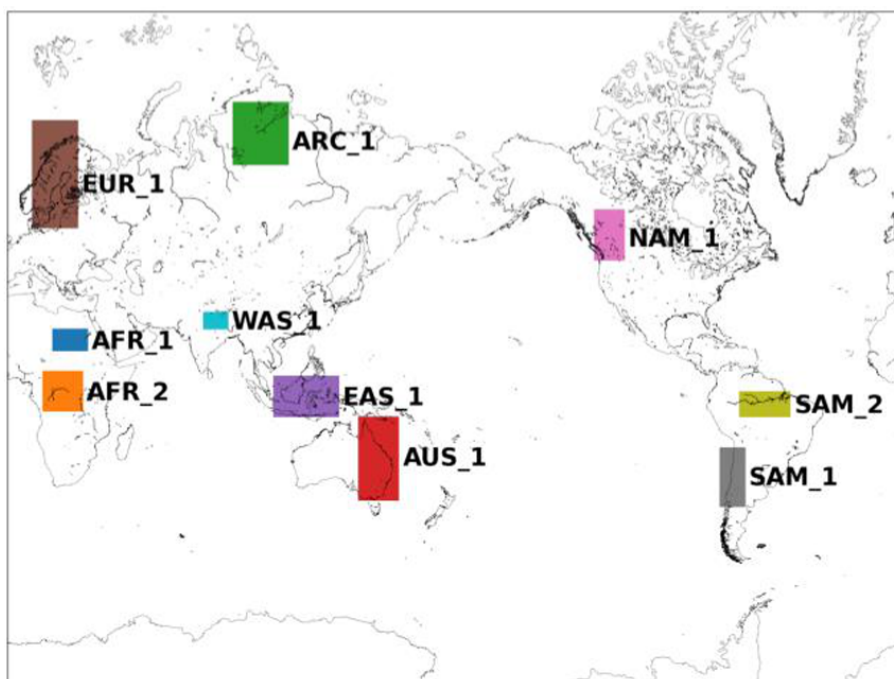


Figure 3. Evaluation domains.

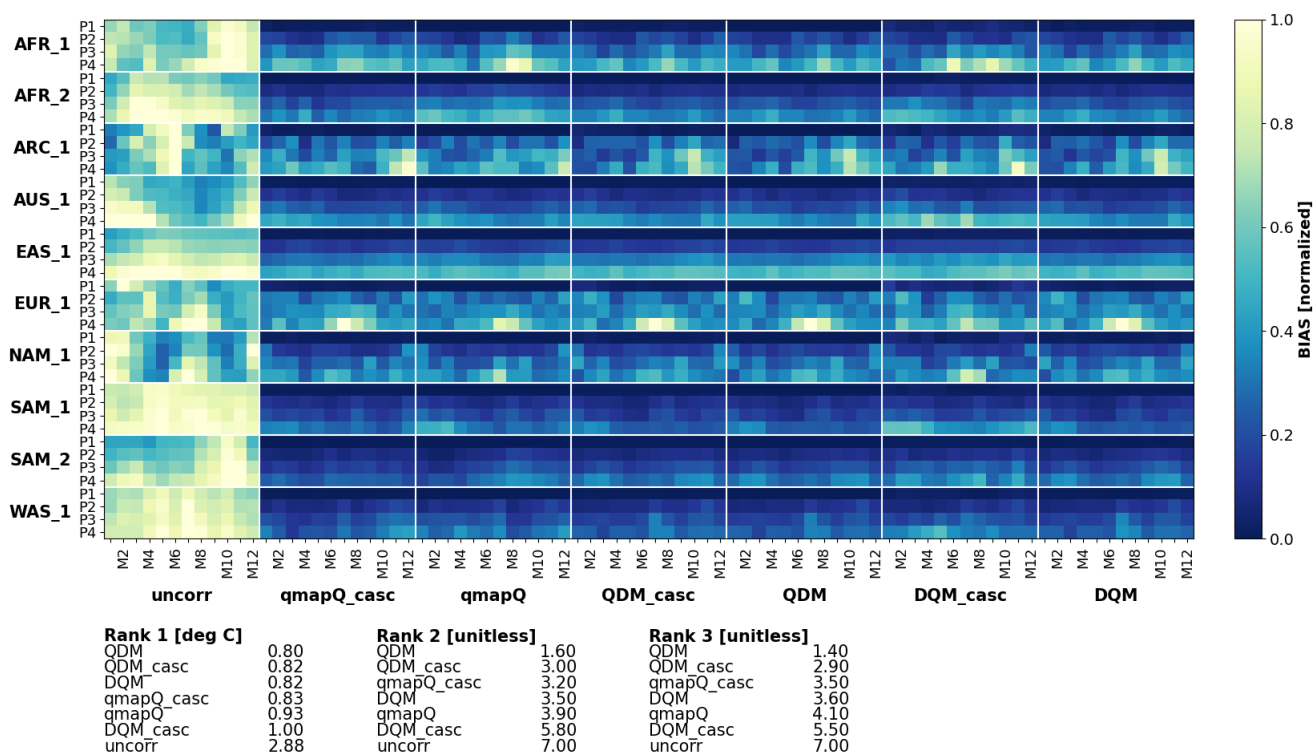


Figure 4. Bias of mean temperature in the original data (uncorr) and after applying the different bias adjustment methods with (subscript "casc") and without temporal cascades. P1–4 mark the evaluation periods 1971–2000 (also calibration period), 2011–2040, 2041–2070, 2071–2100. The results are presented for each of the domains (vertical) and for each month of the year (M1–12). The results are normalised for each sub-panel, i.e. each domain, such that the bias of the uncorrected data and all methods are in the range 0–1.

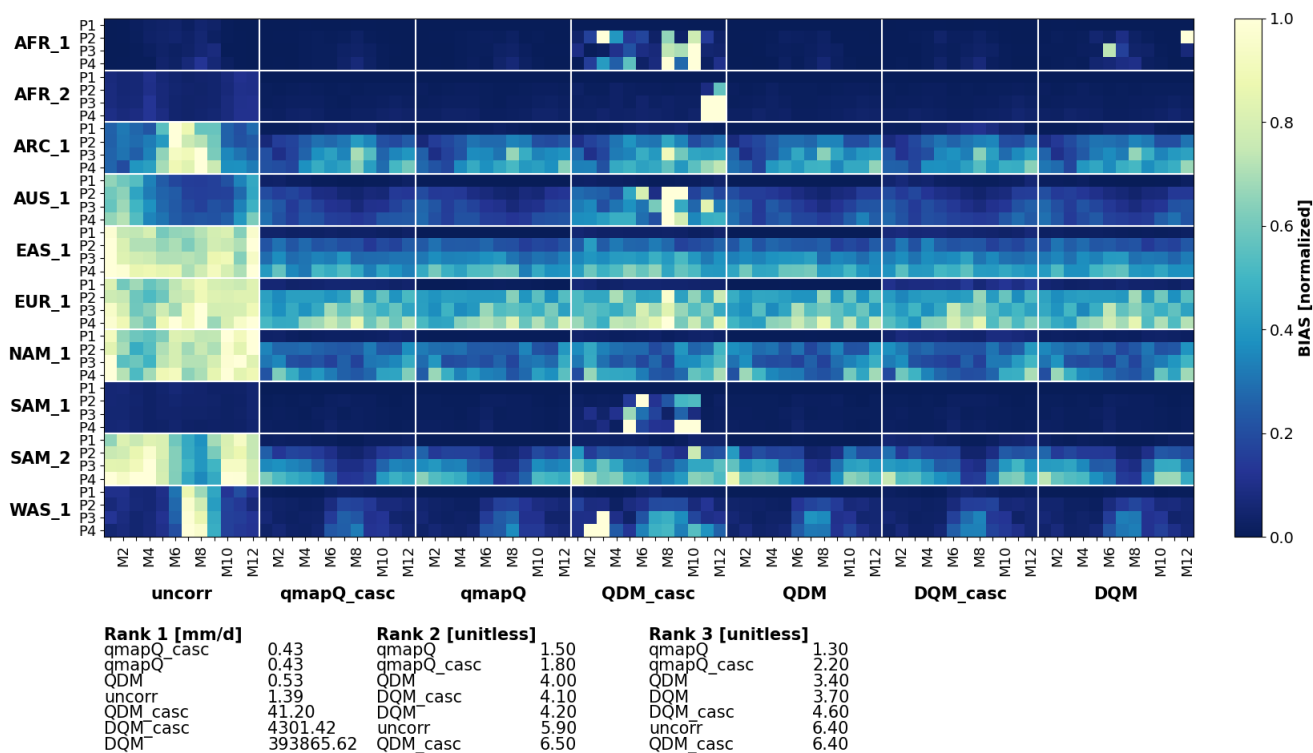


Figure 5. Same as Fig. 4, but for mean precipitation.

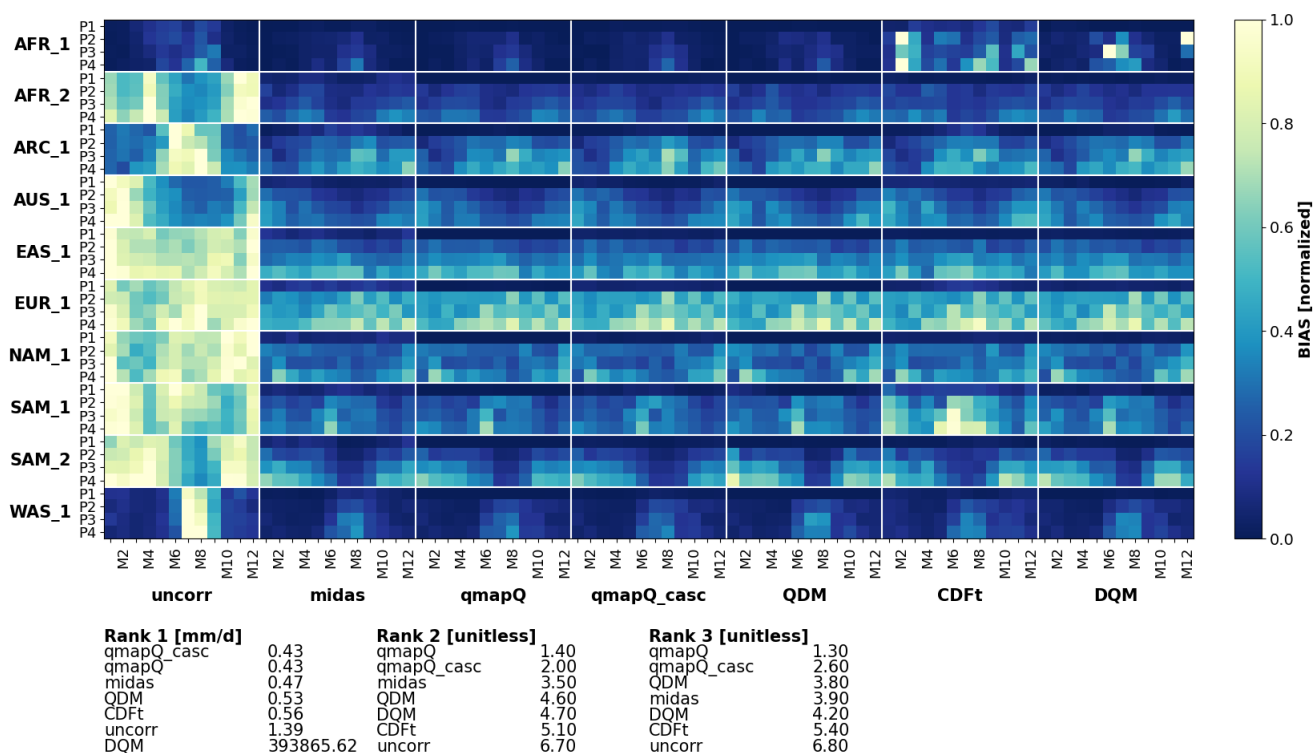


Figure 6. Bias of mean precipitation in the original data (uncorr) and after applying the different bias adjustment methods. P1–4 mark the evaluation periods 1971–2000 (also calibration period), 2011–2040, 2041–2070, 2071–2100. The results are presented for each of the domains (vertical) and for each month of the year (M1–12). The results are normalised for each sub-panel, i.e. each domain, such that the bias of the uncorrected data and all methods are in the range 0–1.

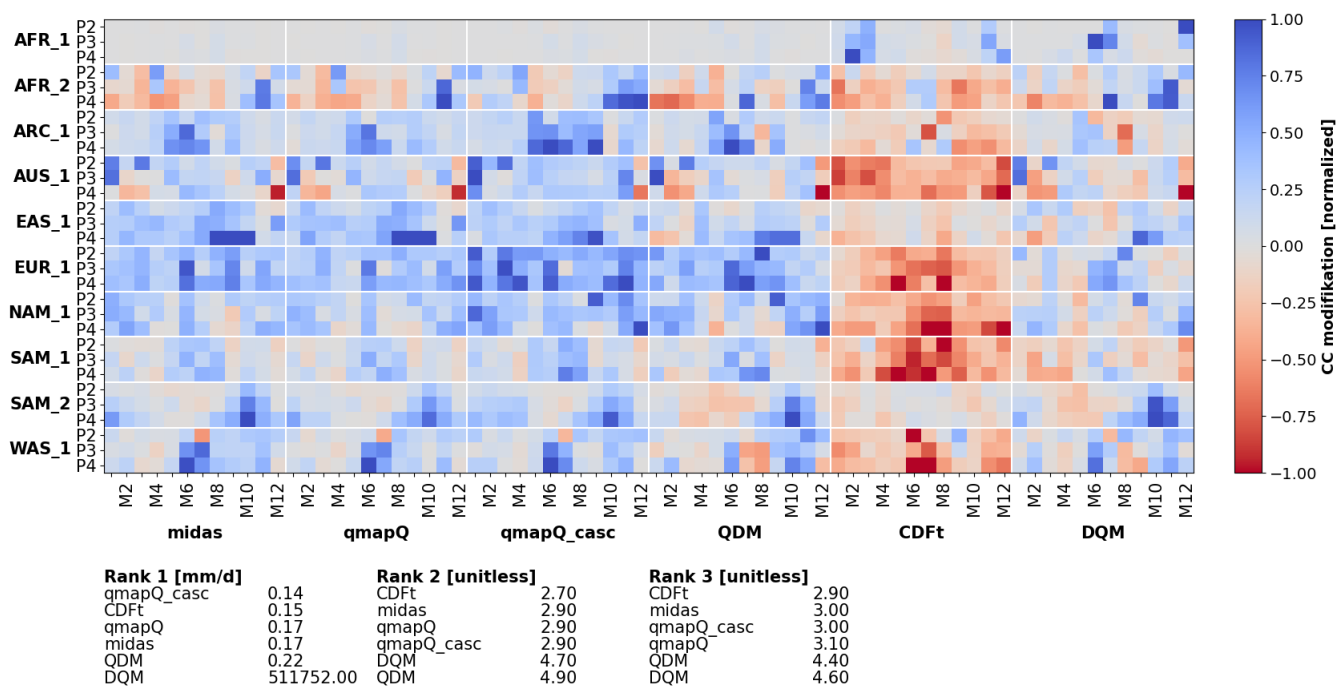


Figure 7. Same as Fig. 6, but for the modification of the climate change signal, and excluding the original data.

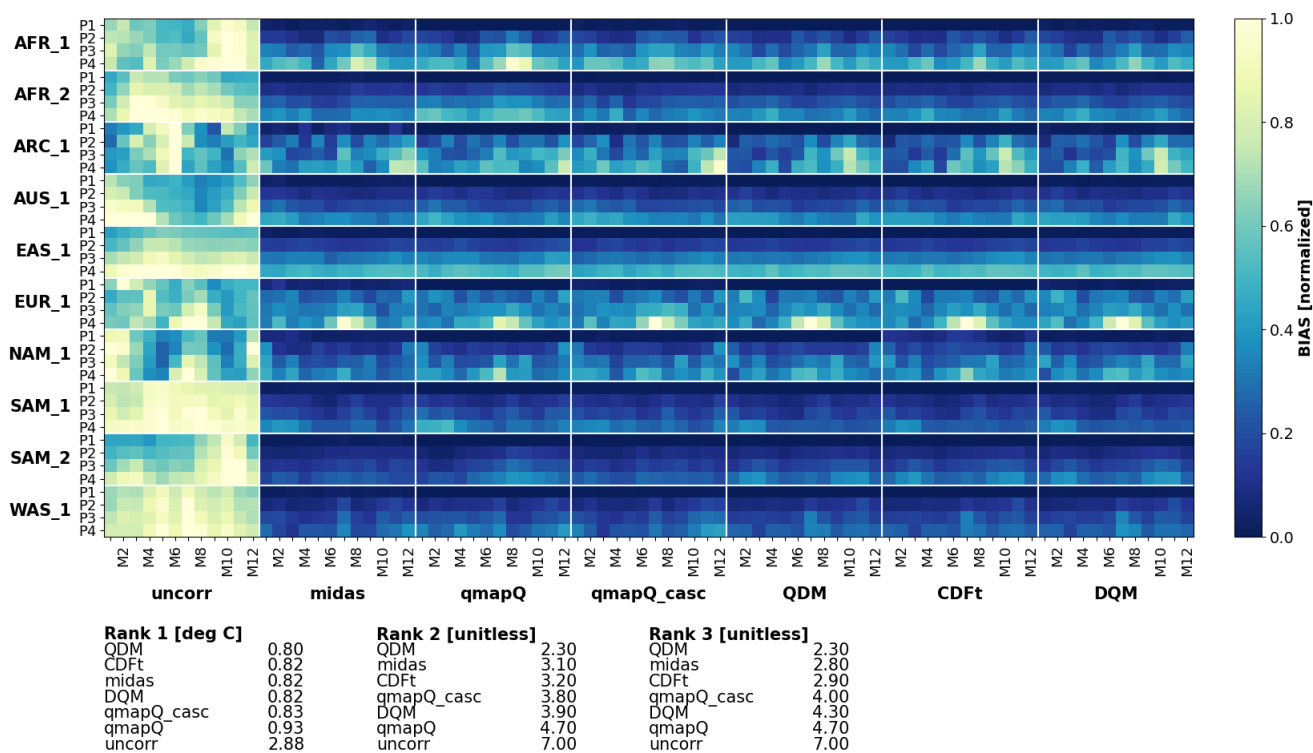


Figure 8. Same as Fig. 6, but for mean temperature.

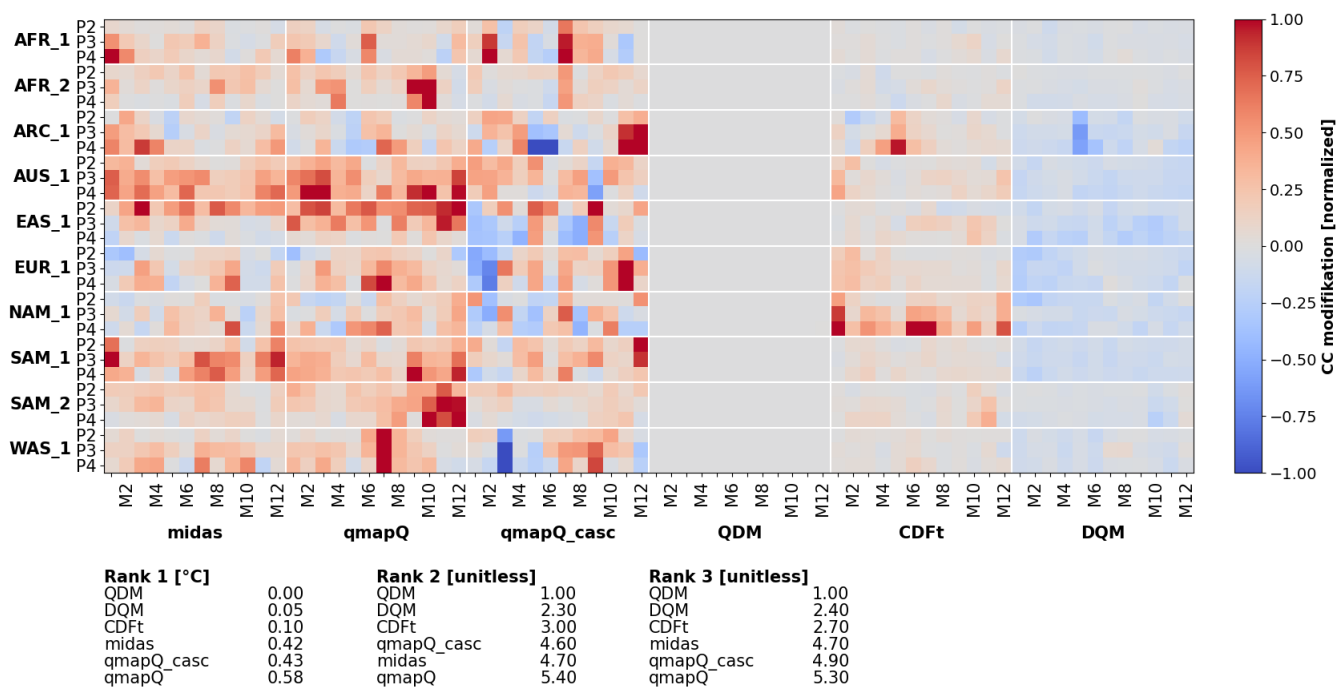


Figure 9. Same as Fig. 7, but for mean temperature.